Pacemaker-neuron–dependent disturbance of the molecular clockwork by a *Drosophila* CLOCK mutant homologous to the mouse *Clock* mutation

Euna Lee[a,b], Eunjoo Cho[c], Doo Hyun Kang[a,b], Eun Hee Jeong[b], Zheng Chen[d], Seung-Hee Yoo[d], and Eun Young Kim (김은영)[a,b,c,1]

[a]Neuroscience Graduate Program, BK21 Plus Program, Department of Biomedical Sciences, Ajou University School of Medicine, Yeongtong-gu, Suwon, Kyunggi-do 16499, Republic of Korea; [b]Department of Brain Science, Ajou University School of Medicine, Yeongtong-gu, Suwon, Kyunggi-do 16499, Republic of Korea; [c]Chronic Inflammatory Disease Research Center, Ajou University School of Medicine, Yeongtong-gu, Suwon, Kyunggi-do 16499, Republic of Korea; and [d]Department of Biochemistry and Molecular Biology, McGovern Medical School, The University of Texas Health Science Center at Houston, Houston, TX 77030

Circadian clocks are composed of transcriptional/translational feedback loops (TTFLs) at the cellular level. In *Drosophila* TTFLs, the transcription factor dCLOCK (dCLK)/CYCLE (CYC) activates clock target gene expression, which is repressed by the physical interaction with PERIOD (PER). Here, we show that amino acids (AA) 657–707 of dCLK, a region that is homologous to the mouse *Clock* exon 19-encoded region, is crucial for PER binding and E-box–dependent transactivation in S2 cells. Consistently, in transgenic flies expressing dCLK with an AA657–707 deletion in the *Clock* (*Clk*[out]) genetic background (p{*dClk-Δ*};*Clk*[out]), oscillation of core clock genes' mRNAs displayed diminished amplitude compared with control flies, and the highly abundant dCLKΔ657–707 showed significantly decreased binding to PER. Behaviorally, the p{*dClk-Δ*};*Clk*[out] flies exhibited arrhythmic locomotor behavior in the photic entrainment condition but showed anticipatory activities of temperature transition and improved free-running rhythms in the temperature entrainment condition. Surprisingly, p{*dClk-Δ*};*Clk*[out] flies showed pacemaker-neuron–dependent alterations in molecular rhythms; the abundance of dCLK target clock proteins was reduced in ventral lateral neurons (LN$_v$s) but not in dorsal neurons (DNs) in both entrainment conditions. In p{*dClk-Δ*};*Clk*[out] flies, however, strong but delayed molecular oscillations in temperature cycle-sensitive pacemaker neurons, such as DN$_1$s and DN$_2$s, were correlated with delayed anticipatory activities of temperature transition. Taken together, our study reveals that the LN$_v$ molecular clockwork is more sensitive than the clockwork of DNs to dysregulation of dCLK by AA657–707 deletion. Therefore, we propose that the dCLK/CYC-controlled TTFL operates differently in subsets of pacemaker neurons, which may contribute to their specific functions.

circadian rhythm | CLOCK | dorsal neuron | lateral neuron | TTFL

Circadian timing systems are composed of cell-autonomous oscillators that enable living organisms to anticipate environmental cyclic changes, thereby orchestrating behavior and physiology throughout the day. The cell-autonomous oscillator contains transcriptional/translational feedback loops (TTFLs) composed of positive and negative molecular components, driving the rhythmic oscillation of gene expression with 24-h periodicity (1, 2). In *Drosophila*, the positive components are the basic helix–loop–helix-containing and Period–Arnt–Sim (PAS)-containing transcription factor dCLOCK (dCLK) and CYCLE (CYC), which form a heterodimer and rhythmically bind to E-box sequences (CACGTC) to activate transcription of clock genes and clock-controlled genes (reviewed in ref. 1). In the core loop of the TTFL, dCLK/CYC transcribes *period* (*per*) and *timeless* (*tim*) genes and the translated PER and TIM proteins form heterodimers and translocate into the nucleus during mid-evening. The PER/TIM heterodimers then physically interact with the dCLK/CYC complex to inhibit

dCLK/CYC-activated transcription. Degradation of PER and TIM proteins by timely controlled posttranslational modifications ultimately releases repression of dCLK/CYC activity, initiating a new transcriptional cycle. In the secondary loop of the TTFL, dCLK/CYC activates transcription of *vrille* (*vri*) and *par domain protein Iε* (*pdp Iε*), and VRI and PDP Iε function to repress and activate transcription of *dClk*, respectively, to increase the robustness of the TTFL (3, 4). Highly conserved molecular mechanisms operate in mammals (reviewed in ref. 5). Mouse CLK (mCLK) and brain and muscle Arnt-like 1 (BMAL1), which are the dCLK and CYC orthologs, activate the transcription of genes in the negative arm of the TTFL, including *mPer1, 2, 3* and *cryptochrome1, 2* (*cry1, 2*). Heterodimeric mPER/mCRY complexes subsequently enter the nucleus to inhibit transcription of their own genes. mCLK/BMAL1 also transcribes the genes encoding nuclear receptors *Rora, b, c* and *Rev-erbα, β*, which activate and repress, respectively the expression of *Bmal1*.

Drosophila displays bimodal peaks of locomotor activity under a standard 12-h/12-h light/dark (LD) photic entrainment condition. Morning and evening peaks of activity occur around dawn and dusk, respectively. In *Drosophila*, ~150 anatomically distinct pacemaker neurons are located in the lateral and dorsal parts of the brain and control respective activity peaks (6–8). The neuropeptide pigment dispersing factor (PDF)-positive large ventral

---

Significance

The circadian clock drives ~24-hour rhythms in behavior and physiology of organisms, and is dependent on transcriptional/translational feedback loops (TTFLs) at the cellular level. Pacemaker neurons in the brain control specific circadian behaviors in response to environmental timing cues such as light and temperature cycles. We show here that flies expressing dCLOCK (dCLK) lacking amino acids 657–707, homologous to the mouse *Clock* mutation, display pacemaker-neuron–dependent disturbance of the molecular clockwork. Specifically, the molecular rhythms in light-sensitive pacemaker neurons were significantly disrupted, but the molecular rhythms in temperature-sensitive pacemaker neurons were robust. Our results suggest that the dCLK-controlled TTFL operates differently in subsets of pacemaker neurons, which contributes to their specific functions, such as differential sensitivity to entraining cues.

lateral neurons (lLN$_v$s) respond to light and play a crucial role in mediating light input from the eyes to regulate arousal, sleep, and the startle response (9–12). Under constant dark conditions after entrainment, morning and evening locomotor activity peaks are controlled by morning oscillators composed of PDF-positive small LN$_v$s (sLN$_v$s) and evening oscillators composed of dorsal lateral neurons (LN$_d$s), a fifth sLN$_v$, and some dorsal neurons (DN$_1$s) (6, 8, 13, reviewed in ref. 14). Besides photic cycles, 12-h/12-h high/low temperature cycles that differ by as little as 2–3 °C can synchronize *Drosophila* behavioral locomotor rhythms and molecular oscillations (15–17). Different pacemakers might be responsible for controlling morning and evening activity peaks under temperature cycles. When photic and temperature cues are both present, LN$_v$s and LN$_d$s are sensitive to photic transition, whereas DN$_1$s, DN$_2$s, DN$_3$s, and lateral posterior neurons are more sensitive to temperature transitions (18). In addition, blue-light photopigment CRY-negative DN$_1$ and CRY-null DN$_2$ are known to play a prominent role in entrainment to temperature cycles (18–21).

Physical interaction between positive and negative circadian factors is crucial for the regulation of circadian transcription (22–28). Here, we provide evidence that a small region of dCLK [amino acids (AA) 657–707], homologous to the peptide sequence encoded by exon 19 of mCLK is crucial for its interaction with PER, although it might not function as the direct binding domain. We show that a mutant of dCLK with this region deleted (dCLK-Δ) exhibited reduced E-box–dependent transcriptional activity in S2 cells. Expression of dCLK-Δ in the *Clk*^{out} genetic background (herein named p{*dClk*-Δ};*Clk*^{out}) rendered flies arrhythmic in the photic entrainment condition. Surprisingly, the levels of dCLK target clock proteins were significantly reduced in LN$_v$s; in comparison, other subsets of clock neurons, such as DNs, were less affected. In addition, p{*dClk*-Δ};*Clk*^{out} flies exhibited anticipatory behavior of temperature

transition, which is correlated with strong yet delayed oscillations of core clock proteins in temperature cycle-sensitive clock neurons, including DN$_1$s and DN$_2$s. Our results suggest that LN$_v$ molecular clockwork is more sensitive than DN molecular clockwork to dysregulation of dCLK by AA657–707 deletion. Taken together, we propose that the dCLK/CYC-controlled TTFL operates differently in subsets of pacemaker neurons despite the same molecular constituents, thereby modulating specific functions of pacemaker neurons, such as sensitivities to various entraining cues.

Results

dCLK Internally Deleted for AA657–707 (dCLK-Δ) Shows Reduced Binding to PER and Transcriptional Activity in S2 Cells. To identify regions of dCLK that are crucial for interaction with PER, we generated a series of dCLK internal deletion mutants (Fig. 1*A*). We performed coimmunoprecipitation analyses and quantified the dCLK–PER interaction by calculating the ratio of pulled-down PER to each immunoprecipitated dCLK variant (Fig. 1 *B* and *C*). The dCLK variant with deletion of AA579–778 (region 10 in Fig. 1*A*) manifested the most severe impairment in binding PER. Previous reports show that the AA657–707 region of dCLK enclosed in AA579–778 is homologous to the 51-aa segment encoded by exon 19 of *mClk*, which is deleted in *Clock/Clock* mutant mice (29, 30) (Fig. 1*A*). Interestingly, the C terminus of apCLK of the silk-moth *Antheraea pernyi* also has a sequence homologous to the exon 19 region in mCLK, and a C-terminal truncation mutant of apCLK complexed with apBMAL1 could not be inhibited by apPER, suggesting the presence of an apPER binding domain in this region (31). Thus, we evaluated whether dCLK AA657–707, which is conserved in all three species, is the minimal region required for PER binding. We generated a deletion mutant of dCLK lacking AA657–707 (dCLK-Δ) and performed coimmunoprecipitation
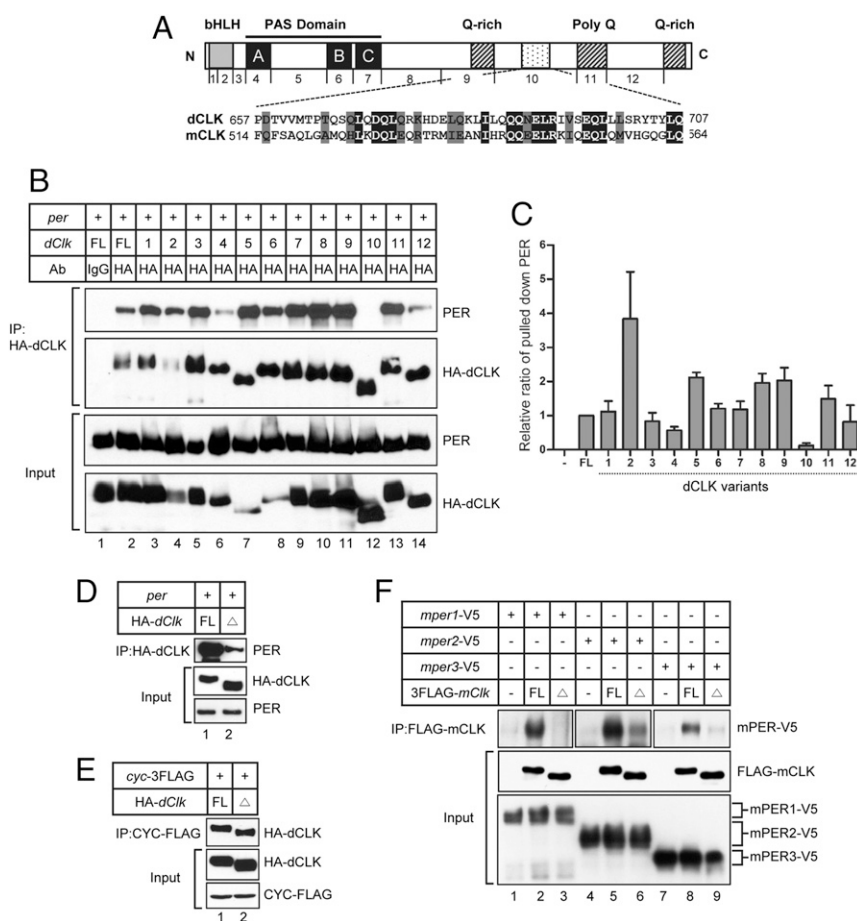
Fig. 1. dCLK subregion encompassing AA657–707 is required for binding with PER. (*A*) Schematic diagram illustrates the protein domains of dCLK. In the alignment between dCLK AA657–707 and mCLK AA514–564, black shading indicates amino acid identity and gray shading indicates conserved substitution. bHLH, basic helix–loop–helix. (*B*) S2 cells were cotransfected with pAct-*per* and pMT-HA-*dClk* (full length, FL) or vectors encoding internally deleted dCLK variant indicated by the numbers 1–12, corresponding to the numbers in the schematic diagram in *A*. Protein extracts (input) were subjected to immunoprecipitation (IP) using anti-HA antibody for dCLK or normal IgG. The immune complexes were analyzed by immunoblotting. (*C*) Relative levels of PER pulled down with each dCLK variant are shown. Values are the mean ± SEM from three independent experiments. (*D*) S2 cells were cotransfected with pAct-*per* and pMT-HA-*dClk* (FL) or pMT-HA-*dClk*Δ657–707 (Δ), and immunoprecipitation was performed as described in *B*. (*E*) S2 cells were cotransfected with pMT-cyc-3F and pMT-HA-*dClk* (FL) or pMT-HA-*dClk*Δ657–707 (Δ). Immunoprecipitation was performed with anti-FLAG antibody, and immune complexes were analyzed by immunoblotting. (*F*) HEK293T cells were transiently cotransfected with pcDNA3-*mper*1-V5, pcDNA3-*mper*2-V5, or pcDNA3-*mper*3-V5 in combination with pCMV10-3FLAG-*mClk* (FL) or pCMV10-3FLAG-*mClk*Δ19 (Δ). Immunoprecipitation was performed with an anti-FLAG antibody, and immune complexes were analyzed by immunoblotting. The immunoblot is representative of three independent experiments.

experiments to assess its ability to interact with PER. The dCLK-Δ showed severely attenuated binding to PER (Fig. 1D), suggesting that this minimal region is required for PER binding. However, dCLK-Δ retained the ability to interact with CYC (Fig. 1E).

Because AA657–707 of dCLK displays significant sequence homology to the 51-aa segment encoded by exon 19 of *mClk*, we next examined whether this domain is also required for interaction between mCLK and the three mPER proteins (mPER1, mPER2, and mPER3). We performed coimmunoprecipitation analyses between either full-length mCLK or mCLK lacking exon 19 (mCLKΔ19) and each mPER homolog in mammalian HEK293 cells (Fig. 1F). Intriguingly, like dCLK-Δ, mCLKΔ19 exhibited impaired interaction with mPER1, mPER2, and mPER3, suggesting that the biochemical feature of interaction between PER and CLK is conserved in flies and mammals.

The exon 19 region of mCLK is crucial for its transcriptional activity (22, 32). Next, we examined whether dCLK-Δ displays compromised transcriptional activity using a luciferase reporter-based assay in S2 cells (22, 28). Transfection of full-length dCLK increased E-box–dependent luciferase expression, whereas dCLK-Δ did not significantly induce luciferase expression (Fig. S1). Given that steady-state levels of ectopically expressed full-length dCLK and dCLK-Δ were similar in S2 cells (Fig. 1 D and E), these results suggest that dCLK-Δ is impaired in transcriptional activation and that AA657–707 of dCLK is essential, not only for PER interaction but also for transcriptional activation in S2 cells.

Next, to examine whether the AA657–707 functions as a direct PER binding domain, we performed an in vitro binding assay using purified GST-tagged dCLK fragments and in vitro transcribed/translated PER (Fig. S2). GST-tagged full-length dCLK, but not dCLK fragments AA80–448, AA579–778, AA657–707, and AA841–956, associated with PER. To our surprise, the AA380–528 fragment strongly associated with PER, suggesting that this region is a novel direct PER binding region (Fig. S2). Therefore, at present, it is not clear which region of dCLK is a direct binding site for PER, but AA657–707 of dCLK is clearly important for interacting with PER and for dCLK transcriptional activity; moreover, this region is homologous to the exon 19 region of mCLK.

p{*dClk*-Δ};*Clk*^out Flies Display Arrhythmic Behavior in the Photic Entrainment Condition. To investigate the in vivo clock function of AA657–707 of dCLK, we generated transgenic flies harboring the *dClk*Δ657–707 transgene. Previous reports have shown that the wild-type version of this transgene fully rescues the arrhythmicity of *Clk*^out flies, which do not express functional dCLK (33, 34) (Fig. 2A and Table 1). Two independent fly lines expressing dCLKΔ657–707 were obtained and switched to the *Clk*^out genetic background [referred to as p{*dClk*-Δ},2M;*Clk*^out and p{*dClk*-Δ},4M;*Clk*^out]. Both p{*dClk*-Δ};*Clk*^out fly lines manifested arrhythmic behaviors (Fig. 2 B and C and Table 1). Interestingly, both p{*dClk*-Δ};*Clk*^out lines displayed little or no morning startled activities; however, evening startled activities were observed, and the flies were pref-
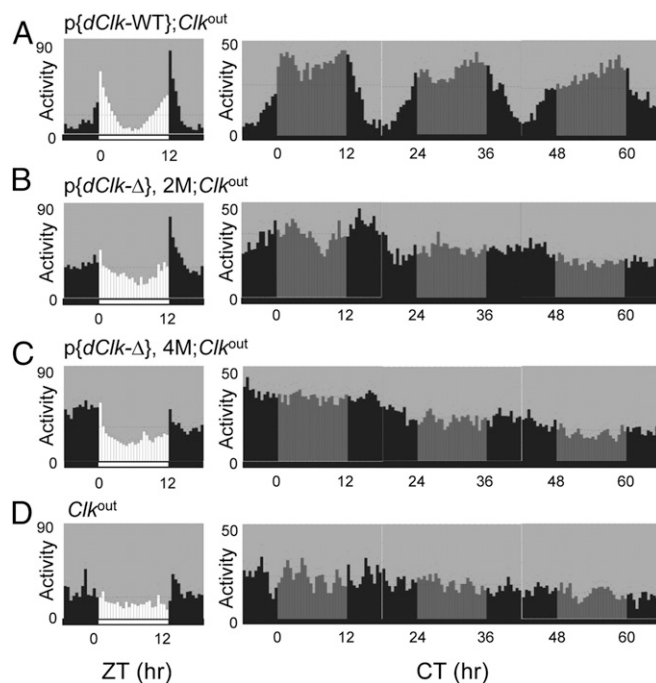

Fig. 2. p{*dClk*-Δ};*Clk*^out flies manifest abnormal locomotor behavior under LD and constant dark (DD) conditions. The locomotor activity of p{*dClk*-WT}; *Clk*^out (A), p{*dClk*-Δ},2M;*Clk*^out (B), p{*dClk*-Δ},4M;*Clk*^out (C), and *Clk*^out (D) fly lines is shown. Each panel represents the average activity of male flies for a given genotype during the 12-h/12-h LD cycle, followed by the DD condition. The white vertical bars represent locomotor activity during the light phase of the LD cycle, and the black vertical bars represent locomotor activity during the dark phase of the LD cycle. The gray vertical bars represent locomotor activity during the subjective light phase of the DD condition. The white horizontal bars and black horizontal bars below each panel indicate 12-h periods of lights-on and lights-off, respectively.

erentially active during the dark phase (Fig. 2 B and C). These daily activity patterns were highly similar to the daily activity patterns of *Clk*^out (Fig. 2D) and *Clk*^Jrk flies, neither of which expresses functional dCLK protein (33–35). Under constant dark conditions, the p{*dClk*-Δ},2M;*Clk*^out flies showed dampened morning and evening activity peaks with delayed phases, whereas the p{*dClk*-Δ},4M;*Clk*^out flies did not manifest evident peaks of activity (Fig. 2 B and C). Thus, we used the p{*dClk*-Δ},4M;*Clk*^out fly line, which showed more severe circadian behavioral defects, for further analyses unless otherwise stated. Taken together, these data clearly indicate that AA657–707 of dCLK is essential in generating circadian locomotor rhythmicity in the photic entrainment condition.

Table 1. Behavioral rhythms of p{*dClk*-Δ};*Clk*^out flies

Genotype	Temperature, °C	No.*	Tau ± SEM, h	Rhythmicity,[†] %	Power[‡]
*w;*p{*dClk*-WT},1A;*Clk*^out	25[§]	32	23.8 ± 0.13	84.4	115.1
*w;*p{*dClk*-Δ},2M;*Clk*^out	25	39	AR	AR	AR
*w;*p{*dClk*-Δ},4M;*Clk*^out	25	30	AR	AR	AR
Clk^out	25	28	AR	AR	AR
*w;*p{*dClk*-WT},1A;*Clk*^out	29/24[#]	28	23.1 ± 0.12	67.8	68.8
*w;*p{*dClk*-Δ},2M;*Clk*^out	29/24	30	24.9 ± 0.44	66.7	74.2

AR, arrhythmic.
*Total number of flies that survived until the end of the testing period.
[†]Percentage of flies with activity rhythms having a power value of ≥10 and a width value of ≥2.
[‡]Measure of the strength or amplitude of the rhythm.
[§]Flies were kept at 25 °C and exposed to 4 d of a 12-h/12-h LD cycle, followed by 7 d of a DD condition.
[#]Flies were kept in constant darkness and exposed to 12-h/12-h temperature cycles of 29 °C/24 °C for 6 d, followed by 7 d of constant 24 °C.
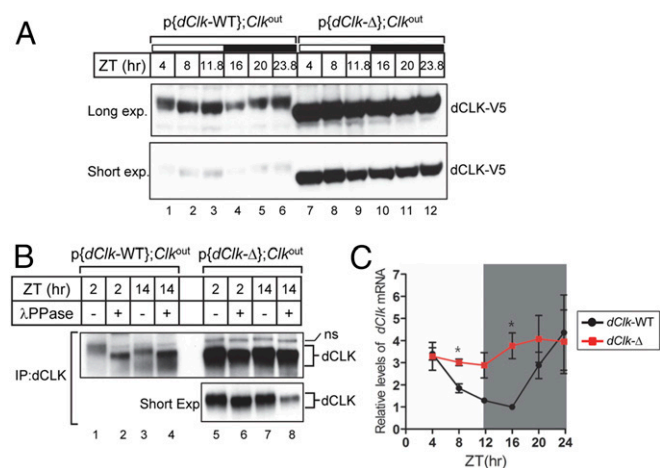
Fig. 3. Daily oscillation of dCLK protein and mRNA levels is altered in p{dClk-Δ};Clk^out flies. Adult flies of the indicated genotype were collected at the indicated times of the day (ZT). Head protein extracts were prepared and analyzed by immunoblotting with an anti-V5 antibody (A) or by immunoprecipitation with anti-dCLK antibody (gp208) (B). Immune complexes were further incubated in the absence (−) or presence (+) of λ-phosphatase (λPPase) and immunoblotted with anti-dCLK antibody (gp208). Results of short and long exposure (Exp) of the dCLK Western blot are shown. ns, nonspecific. (C) Total RNA was obtained to perform quantitative real-time PCR. Relative levels of dClk mRNA were quantified. Values represent mean ± SEM from three independent experiments. Asterisks indicate statistically significant difference between values at each time point (Student's t test: *P < 0.05).

p{dClk-Δ};Clk^out Flies Exhibit Altered Molecular Rhythms. To delineate the in vivo functions of dCLK AA657–707, we analyzed the molecular rhythms of p{dClk-Δ};Clk^out flies under a 12-h/12-h LD cycle. In control p{dClk-WT};Clk^out flies, dCLK-WT protein manifested daily changes in phosphorylation as reported previously (33, 36, 37) (Fig. 3 A and B). In contrast, in p{dClk-Δ};Clk^out flies, hyperphosphorylated isoforms of dCLK were absent or diminished (Fig. 3 A and B). This result is consistent with the notion that AA657–707 is required for PER binding, and consequently recruiting DBT to induce dCLK hyperphosphorylation (28, 36–39). Nonetheless, slight changes in mobility shift were observed from λ-phosphatase–treated dCLK-Δ at zeitgeber time (ZT) 2, which suggested either that DBT recruited by PER at an attenuated level or that other kinase(s) mediates residual phosphorylation of dCLK-Δ (Fig. 3B, compare lanes 5 and 6). In agreement with a previous report showing that hyperphosphorylated dCLK isoforms are sensitive to degradation, levels of dCLK-Δ were higher than levels of dCLK-WT (Fig. 3A). Amplitude of the daily oscillation in dClk-Δ mRNA levels was markedly dampened compared with amplitude of the daily oscillation of dClk-WT (Fig. 3C). This decreased amplitude was mainly because of the increased trough levels during midday, likely resulting from downregulation of VRI, a repressor of dClk transcription (3) (Fig. 4C). Together, these data demonstrate that both transcriptional and posttranslational regulation contribute to the increased levels of dCLK-Δ (Fig. 3A).

To examine the molecular clockwork defects in p{dClk-Δ};Clk^out flies further, we next measured daily oscillations in the mRNA and protein levels of dCLK target clock genes in the LD cycle. Consistent with the low transcriptional activation by dCLK-Δ observed in S2 cells (Fig. S1), the mRNA levels of the dCLK-CYC target genes tim, per, and vri were significantly reduced throughout the day in p{dClk-Δ};Clk^out flies compared with the mRNA levels of those genes in p{dClk-WT};Clk^out flies (Fig. 4 A–C). Nonetheless, p{dClk-Δ};Clk^out flies showed daily oscillation of tim, per, and vri expression, albeit with low amplitude and phase delay, implying that dCLK-Δ/CYC retains residual transcriptional activity. Although not statistically significant, the dCLK-CYC target gene mRNA levels of p{dClk-Δ};Clk^out flies late at night (ZT24) were

reproducibly higher than mRNA levels of p{dClk-WT};Clk^out flies. In addition, the rates of decrease in mRNA levels were slower in p{dClk-Δ};Clk^out flies than in control flies. These results are consistent with the notion that PER inhibition of dCLK-Δ/CYC-dependent transcription is attenuated in p{dClk-Δ};Clk^out flies due to the weak association of PER and dCLK-Δ (Figs. 1D and 5).

Next, overall daily levels of TIM and PER proteins in p{dClk-Δ};Clk^out flies were comparable to the daily levels of those proteins in p{dClk-WT};Clk^out flies (Fig. 4 D–G). However, moderate changes were observed in TIM and PER cycling in p{dClk-Δ};Clk^out flies. The rate of TIM accumulation between ZT8 and ZT12 was slower than the rate of TIM accumulation in control flies, possibly due to low tim mRNA levels. Although TIM levels began to decrease sharply at ZT20 in p{dClk-WT};Clk^out flies, they were maintained at peak levels until ZT24 in p{dClk-Δ};Clk^out flies (Fig. 4 D and F), suggesting that TIM degradation is reduced in p{dClk-Δ};Clk^out flies at night. Similarly, in p{dClk-Δ};Clk^out flies, the rate of PER accumulation was slow compared with the rate of PER accumulation in p{dClk-WT};Clk^out flies (Fig. 4 E and G). Moreover, whereas PER levels had already decreased by ZT24 in p{dClk-WT};Clk^out flies, PER accumulation continued until ZT24 in p{dClk-Δ};Clk^out flies (Fig. 4G), likely due to the increased level of TIM, which protects PER from phosphorylation and degradation (40, 41).

Next, we measured tim and per mRNA and protein levels in constant dark conditions. In p{dClk-Δ};Clk^out flies, tim and per mRNA levels were greatly reduced and the amplitudes of rhythmic oscillation were markedly dampened (Fig. S3 A and B). The upswing of tim and per expression was greatly dampened during
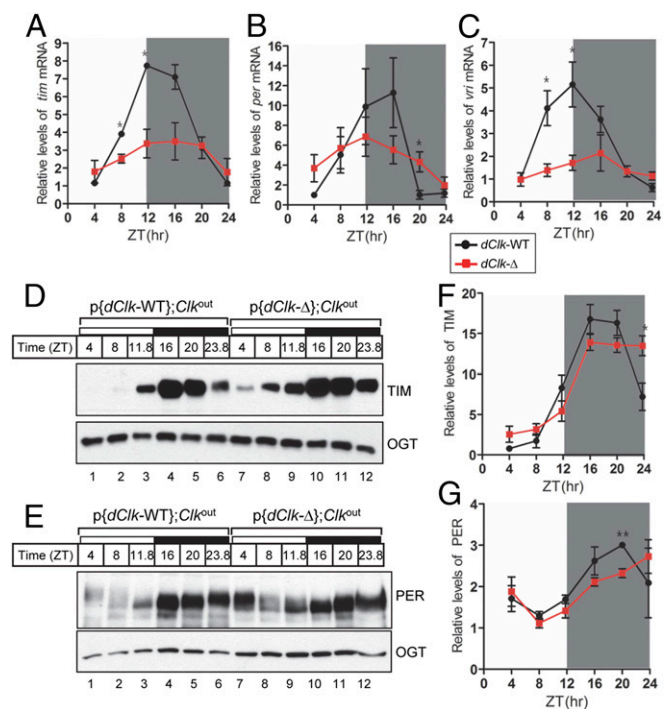

Fig. 4. Daily oscillation of dCLK target protein and mRNA levels is altered in p{dClk-Δ};Clk^out flies. Adult flies of the indicated genotype were collected at indicated times of the day. (A–C) Total RNA was obtained to perform quantitative real-time PCR. Relative levels of tim (A), per (B), or vri (C) mRNA were quantified. (D and E) Head protein extracts were prepared, and Western blot analysis was performed using anti-TIM or anti-PER antibody. O-GlcNAc transferase (OGT) served as a loading control. (F and G) Relative levels of TIM and PER protein were determined by measuring band intensities using ImageJ software (NIH). Values represent mean ± SEM from three independent experiments. Asterisks indicate statistically significant difference between values at each time point (Student's t test: *P < 0.05; **P < 0.01).
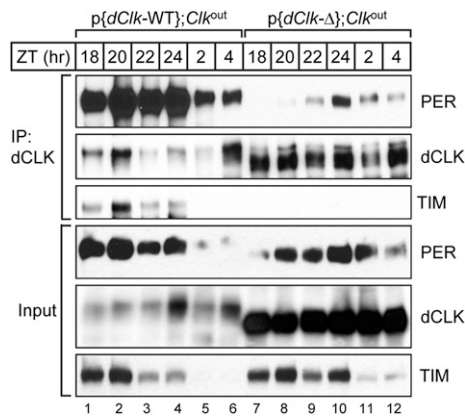
Fig. 5. Interaction between dCLK-Δ and PER is reduced in p{dClk-Δ};Clk[out] flies. Adult flies of the indicated genotype were collected at the indicated times of day. Head protein extracts were prepared and directly analyzed by immunoblotting (input) or processed for immunoprecipitation with an anti-dCLK antibody (gp208). Immune complexes were analyzed by immunoblotting with anti-PER, anti-dCLK, or anti-TIM antibody.

which ultimately affects PER stability (42–45). Accordingly, molecular oscillations of *per/tim* mRNAs and proteins were rapidly dampened in the absence of light, leading to behavioral arrhythmicity in constant dark conditions.

dCLK-Δ Shows Impaired Binding to PER and TIM in Flies. To ascertain that the AA657–707 region of dCLK is required for PER binding in vivo, we performed immunoprecipitation assays with fly head extracts. In control p{dClk-WT};Clk[out] flies, dCLK-WT stably interacted with PER at all time points tested (Fig. 5), as previously reported (23, 28). In sharp contrast, the amount of PER pulled down with dCLK-Δ was greatly reduced (Fig. 5), even though dCLK-Δ levels in the input were much higher than dCLK-WT levels [Fig. 5, immunoprecipitation (IP) and Input, second and fifth rows]. This result indicated that the AA657–707 region is indeed required for PER binding in flies. We previously reported that TIM complements the binding between dCLK and PERΔCLK binding domain (PERΔCBD), a PER lacking the dCLK binding domain (28). To explore whether TIM contributes to the binding of dCLK-Δ to PER, we probed immune complexes pulled down with anti-dCLK antibodies for the presence of TIM (Fig. 5, IP, third row). Surprisingly, TIM was not detected in the dCLK-Δ-containing immune complexes, indicating that AA657–707 is also important for the interaction of dCLK with TIM.

The dCLK Target Clock Protein Levels Are Reduced in LN_vs of p{dClk-Δ}; Clk[out] Flies. To understand better the strong behavioral defects of p{dClk-Δ};Clk[out] flies, we analyzed clock protein oscillations in fly brain pacemaker neurons by immunohistochemistry. Inspection of anti-PDF immunofluorescence revealed no apparent anatomical defects in the PDF-positive neurons in p{dClk-Δ};Clk[out] flies compared with the PDF-positive neurons in p{dClk-WT};Clk[out] flies (Fig. 6A). TIM in p{dClk-WT};Clk[out] flies showed robust oscillation in terms of levels and subcellular localization in pacemaker neurons (Fig. 6A, *Top*). In comparison, whereas temporal staining patterns of TIM in p{dClk-Δ};Clk[out] flies were similar to temporal staining patterns of control flies, we noted important differences (Fig. 6A, *Bottom*). Specifically, although comparable TIM signal intensities were detected from LN_ds, DNs, and other cells, TIM
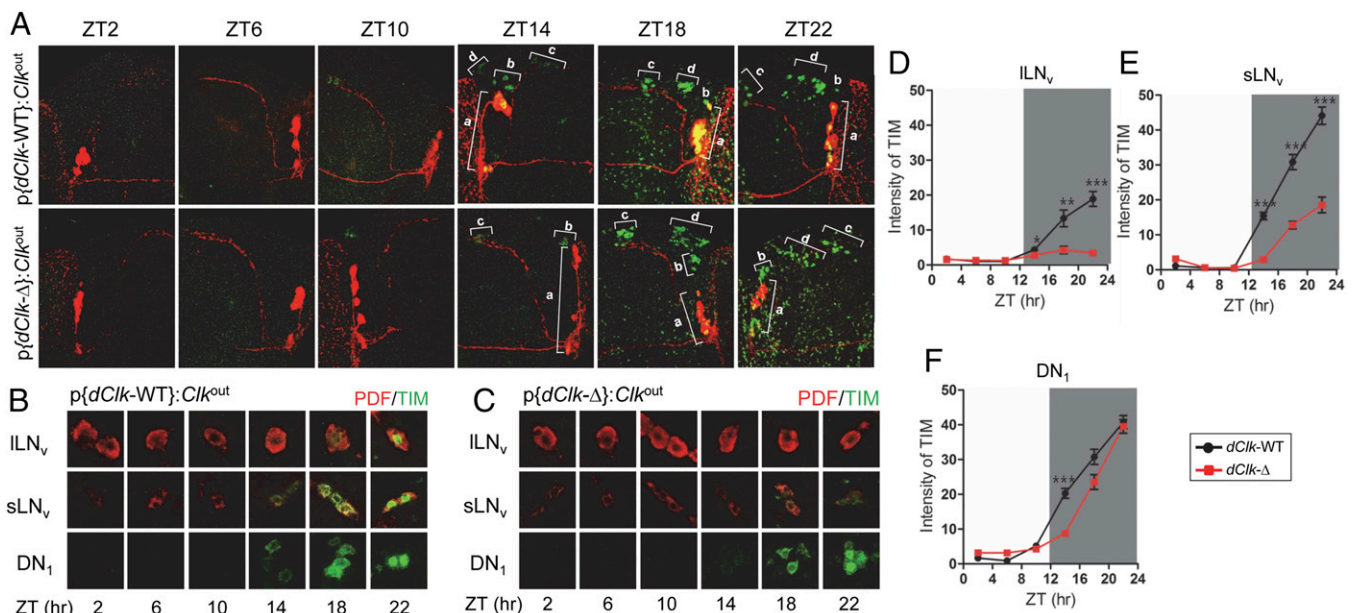
the subjective day, presumably due to the persistent repression of dCLK-Δ/CYC by elevated levels of PER until circadian time (CT) 8 (discussed below). In p{dClk-Δ};Clk[out] flies, TIM levels were significantly higher than in p{dClk-WT};Clk[out] flies during the subjective early morning (CT4 and CT8) and slowly reached the peak at CT20, although at a much reduced level compared with p{dClk-WT};Clk[out] flies (Fig. S3 *C and D*). Similarly, PER levels were markedly higher with concomitant increases in hyperphosphorylated isoforms during the subjective early morning (CT4 and CT8), probably due to the high levels of TIM protecting PER from phosphorylation and degradation in p{dClk-Δ};Clk[out] flies (Fig. S3 *C and E*). Taken together, these results suggest that quasi-normal oscillations of PER and TIM proteins in fly heads in the LD cycle are mainly driven by light-mediated degradation of TIM,

Fig. 6. TIM protein levels are significantly reduced in LN_vs of p{dClk-Δ};Clk[out] flies. Adult flies of the indicated genotype were collected at the indicated times of day, and isolated brains were processed for whole-mount immunohistochemistry. Brains were costained for TIM (green) and PDF (red). (A) Stained images were obtained under a 40× objective, and confocal sections were combined. a, lLN_vs and sLN_vs; b, LN_ds; c, DN_1s; d, DN_3s. Confocal images were obtained under a 63× objective (B and C), and TIM fluorescence intensity was quantified (D–F). Images are representative for each subset of pacemaker neurons. Values represent mean ± SEM (n = 16–50). Asterisks indicate statistically significant difference between values at each time point (Student's *t* test: *P < 0.05; **P < 0.01; ***P < 0.001).
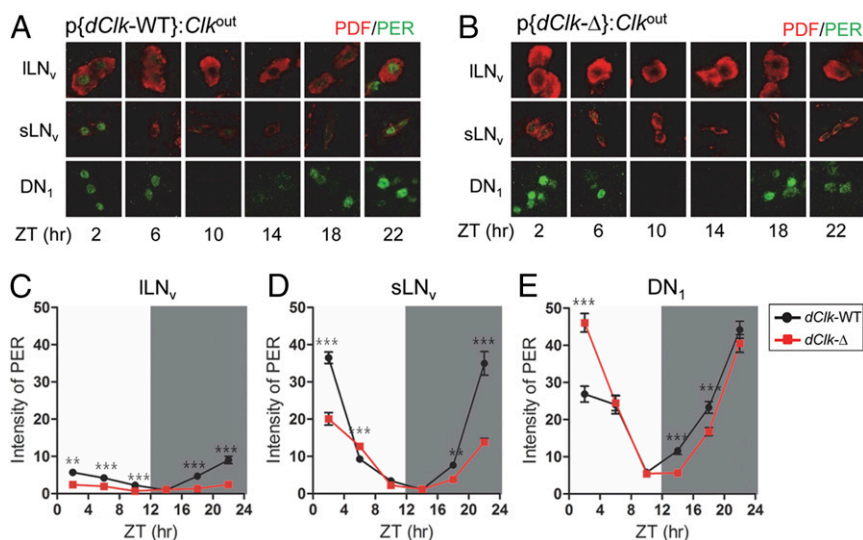
Fig. 7. PER protein levels are significantly reduced in LN$_v$s of p{dClk-Δ};Clk^{out} flies. Adult flies of the indicated genotype were collected at the indicated times of day, and isolated brains were processed for whole-mount immunohistochemistry. Confocal images of brains costained for PER (green) and PDF (red) were obtained under a 63× objective (A and B), and PER fluorescence intensity was quantified in each subset of pacemaker neurons (C–E). Images are representative for each subset of pacemaker neurons. Values represent mean ± SEM (n = 16–50). Asterisks indicate statistically significant difference between values at each time point (Student's t test: **P < 0.01; ***P < 0.001).

signal was greatly reduced in large LN$_v$s (lLN$_v$s) and small LN$_v$s (sLN$_v$s) in p{dClk-Δ};Clk^{out} flies (Fig. 6A). To verify that TIM levels were differentially affected in subsets of pacemaker neurons in p{dClk-Δ};Clk^{out} flies, we examined TIM staining at a higher magnification in sLN$_v$s, lLN$_v$s, and DN$_1$s at 4-h intervals beginning at ZT2 and quantified TIM signal intensity (Fig. 6 B–F). As expected, TIM levels were greatly reduced in LN$_v$s, with more severe effects from lLN$_v$s than sLN$_v$s at all time points throughout the day (Fig. 6 D and E). In contrast, TIM signal intensity in DN$_1$s was comparable between p{dClk-WT};Clk^{out} flies and p{dClk-Δ};Clk^{out} flies, albeit with slightly attenuated TIM accumulation (Fig. 6F). To determine whether the reduced TIM staining is due to delayed accumulation of TIM, we further analyzed TIM staining intensity at ZT24 and obtained similar results showing reduced TIM intensity in LN$_v$s, but not in LN$_d$s or DN$_1$s, of p{dClk-Δ};Clk^{out} flies (Fig. S4 A and B). Finally, to exclude the possibility that these striking pacemaker-neuron–dependent differences in TIM staining intensity were due to differences in genetic background, we next examined TIM staining in the other p{dClk-Δ};Clk^{out} transgenic fly line (2M) (Fig. S5). Both lines of p{dClk-Δ};Clk^{out} flies exhibited similarly reduced TIM staining in LN$_v$s, but not in DN$_1$s, compared with p{dClk-WT};Clk^{out} flies, indicating that genetic background is not the cause of the observed phenotype.

Next, to examine whether these pacemaker-neuron–dependent differences were specific to TIM, we scored the expression patterns of PER, a state variable of the *Drosophila* circadian clock. Similar to our observations of TIM expression, PER levels were greatly reduced in sLN$_v$s and lLN$_v$s, but not in DN$_1$s, at all time points tested in p{dClk-Δ};Clk^{out} flies compared with p{dClk-WT};Clk^{out} flies (Fig. 7 A–E). Finally, we examined VRI level at ZT17, a time when VRI maintains its maximum level (4). Similar to our observations of PER and TIM, VRI levels were greatly reduced in LN$_v$s but were unchanged in DN$_1$s of p{dClk-Δ};Clk^{out} flies compared with p{dClk-WT};Clk^{out} flies (Fig. S6). In conclusion, all of the evaluated dCLK direct targets exhibited similar pacemaker-neuron–dependent alterations in abundance in p{dClk-Δ};Clk^{out} flies. Interestingly, we sometimes observed a slight reduction in clock protein staining intensity in LN$_d$s of p{dClk-Δ};Clk^{out} flies (Figs. S5 and S6). It is possible that the molecular clockwork in LN$_d$s of p{dClk-Δ};Clk^{out} flies is also disrupted, but to a lesser extent than in LN$_v$s.

p{dClk-Δ};Clk^{out} Flies Display Anticipatory Behavior and Free-Running Rhythms in the Temperature Entrainment Condition. DN$_1$s and DN$_2$s play a prominent role in entrainment to temperature cycles (18–21). Because we found that dCLK target proteins were not reduced in DN$_1$s of p{dClk-Δ};Clk^{out} flies (Figs. 6 and 7), we hypothesized that quasi-normal expression of dCLK target proteins in DNs would allow behavioral synchronization to temperature cycles in p{dClk-Δ};Clk^{out} flies, despite their severe defects in entrainment to photic cycles (Fig. 2). Flies were kept in constant light to wipe out residual behavioral rhythms and then in constant darkness with 12-h/12-h temperature cycles of 29 °C/24 °C. As previously reported, the control p{dClk-WT};Clk^{out} flies exhibited bimodal peaks of activity with an anticipatory activity increase before the temperature transition, similar to what was observed for the photic cycles (15, 19, 33) (Fig. 8 A and B). Indeed, although the p{dClk-Δ};Clk^{out} flies did not manifest any anticipatory activity of the LD transition, they clearly exhibited anticipatory activity of the temperature transition; however, they showed a delayed phase of evening activity compared with the control flies (Fig. 8 C and D). Interestingly, the locomotor activity of p{dClk-Δ};Clk^{out} flies was not strongly suppressed during the initial exposure to constant light, unlike the control flies, which showed substantially suppressed locomotor activity (Fig. 8 A and C). Together with the data showing insignificant dark-to-light startle response of p{dClk-Δ};Clk^{out} flies (Fig. 2 B and C), these data indicate that the light-driven masking effects are reduced in p{dClk-Δ};Clk^{out} flies (46, 47).

To examine whether the delayed phase of evening locomotor activity in p{dClk-Δ};Clk^{out} flies is correlated with molecular oscillations in temperature cycle-sensitive pacemaker neurons, we performed immunohistochemical analysis with anti-PDF and anti-TIM antibodies. In control p{dClk-WT};Clk^{out} flies, TIM levels exhibited a large amplitude of oscillation in each subset of pacemaker neurons, with the exception of lLN$_v$s peaking at ZT14 (Fig. 8 E–J), which is earlier than observed under photic cycle conditions (17, 19, 21, 48). In p{dClk-Δ};Clk^{out} flies, TIM levels in both lLN$_v$s and sLN$_v$s were greatly reduced compared with those TIM levels in p{dClk-WT};Clk^{out} flies (Fig. 8 G and H), similar to the results obtained for the photic cycle. In sharp contrast, TIM levels in DN$_1$s and DN$_2$s of p{dClk-Δ};Clk^{out} flies showed rhythmic oscillation at levels comparable to the TIM levels of control p{dClk-WT};Clk^{out} flies, but the oscillation phases were delayed (Fig. 8 I and J). The alterations in the PER
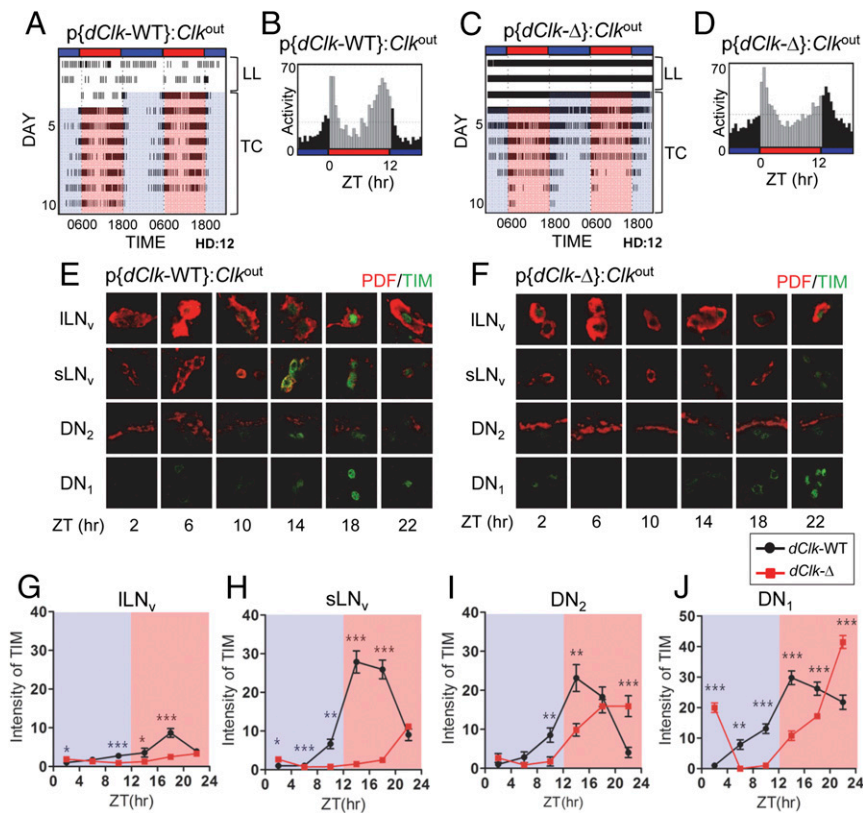
Fig. 8. Behavioral and molecular rhythms of p{dClk-Δ}; Clk[out] flies under temperature cycle conditions. Adult p{dClk-WT};Clk[out] and p{dClk-Δ};Clk[out] flies were first exposed to continuous light (LL) for 2.7 d and entrained to 12-h/12-h temperature cycles (TC) of 29 °C/24 °C in the dark. (*A* and *C*) Vertical black bars in each row of the actogram represent fly activity. The red and blue horizontal bars indicate thermo- and cryo-phases, respectively. HD, hash density. (*B* and *D*) Daily activity profiles of each fly genotype are shown. (*E* and *F*) At the indicated times in the temperature cycle, isolated brains were processed for whole-mount immunohistochemistry. Confocal images of brains costained for TIM (green) and PDF (red) were obtained under a 63× objective. Representative images for each subset of pacemaker neurons are shown. (*G–J*) TIM fluorescence intensity was quantified. Values represent mean ± SEM (*n* = 20–52). Asterisks indicate statistically significant difference between values at each time point (Student's *t* test: *P < 0.05; **P < 0.01; ***P < 0.001).

profile of p{*dClk-Δ*};*Clk*[out] flies were similar to the alterations in the TIM profile. Specifically, in p{*dClk-WT*};*Clk*[out] flies, PER levels were reduced in lLN_vs and sLN_vs, with greater reduction in lLN_vs, but were comparable in DN_1s, where they showed large amplitudes of oscillation but with delayed phases compared with p{*dClk-WT*};*Clk*[out] flies (Fig. S7). Therefore, it is possible that strong but delayed molecular oscillations of core clock proteins in the temperature cycle-sensitive clock neurons drive rhythmic locomotor activity with delayed phase in p{*dClk-Δ*};*Clk*[out] flies.

To examine whether the temperature transition of p{*dClk-Δ*};*Clk*[out] flies was indeed presented by synchronized circadian clock machinery, we analyzed rhythmicity after releasing into a constant temperature. Because the locomotion of p{*dClk-Δ*},4M;*Clk*[out] flies decreased greatly toward the end of the temperature cycle, accompanied by increased mortality for unidentified reasons, we were only able to obtain behavioral results from p{*dClk-Δ*}, 2M;*Clk*[out] flies. Consistent with their advanced phase of evening activity during temperature cycles, the control flies manifested a 23.1-h period in the temperature cycle and showed decreased rhythmicity compared with the photic cycles (Fig. 9 *A* and *C* and Table 1). Importantly, p{*dClk-Δ*},2M;*Clk*[out] flies exhibited 67% rhythmicity with a 24.9-h period, demonstrating that their circadian rhythmicity was enhanced under the temperature entrainment condition, which was in sharp contrast to their arrhythmic behavior under the photic entrainment condition (Table 1). Because the flies were entrained to temperature cycles in the dark, the switch from constant light exposure to dark might have impinged on the clock machinery, resulting in the improved behavioral rhythmicity (49). To examine whether improved behavioral rhythmicity in the temperature entrainment condition in p{*dClk-Δ*},2M;*Clk*[out] flies was due to earlier light exposure, we performed photic entrainment behavioral analysis by exposing the flies to 2 d of constant light before the LD cycle (Table S1). Even with the initial exposure to continuous light before the LD cycle, the behavioral rhythmicity of p{*dClk-Δ*};*Clk*[out] flies was still very poor in the photic entrainment condition. Collectively, we conclude that the behavioral rhythmicity of p{*dClk-Δ*};*Clk*[out] flies is indeed enhanced by temperature cycle entrainment.

Discussion

In *Drosophila*, the cell-autonomous circadian clock is generated by dCLK/CYC-induced transcriptional activation, followed by PER repression of dCLK/CYC-dependent transcription, which constitutes the core TTFL. Here, we show that dCLK AA657–707, which is homologous to the region encoded by exon 19 that is absent in the *Clk/Clk* mutant mouse, is essential for its interaction with PER in S2 cells and flies. Flies expressing dCLK lacking this region in the *Clk*[out] genetic background showed LN_v-specific down-regulation of dCLK target clock proteins and completely arrhythmic locomotor behavior under the photic entrainment condition. On the contrary, expression of dCLK target proteins in other pacemaker neurons, such as DN_1s, was quasi-normal, contributing to anticipatory behavior and improved free-running rhythms under the temperature entrainment condition.

In this study, we demonstrate that AA657–707, enclosed in AA579–778 is essential for interaction with PER (Fig. 1); however, our data also suggest that this region may not function as a direct PER binding domain. In vitro binding assays performed with GST-tagged dCLK fragments showed that PER binds strongly to the central region of dCLK encompassing AA380–528 (Fig. S2). Nonetheless, the extent of interaction between dCLKΔ379–479 (region 8 in Fig. 1*A*) or dCLKΔ480–578 (region 9 in Fig. 1*A*) and PER was increased in the immunoprecipitation analyses in S2 cells (Fig. 1 *B* and *C*). Therefore, it seems likely that the PER interaction domain on dCLK consists of multiple contact sites and that deletion of only some of these sites (e.g., region 8, region 9) does not eliminate the PER binding. In addition, although dCLK internally deleted for PAS-A (region 4 in Fig. 1*A*) showed slightly reduced interaction with PER compared with full-length dCLK, the GST-tagged PAS domain-containing fragment (AA80–448) did not strongly associate with PER. Presumably, the PAS region of dCLK functions in CYC interaction, as in the case of mCLK and BMAL1 (50). In this study, because we sought to examine the in vivo functional outcomes of using (dCLK-Δ) in the molecular clockwork, a mutation that showed decreased PER binding and transcriptional activation, we did not further map the direct PER binding
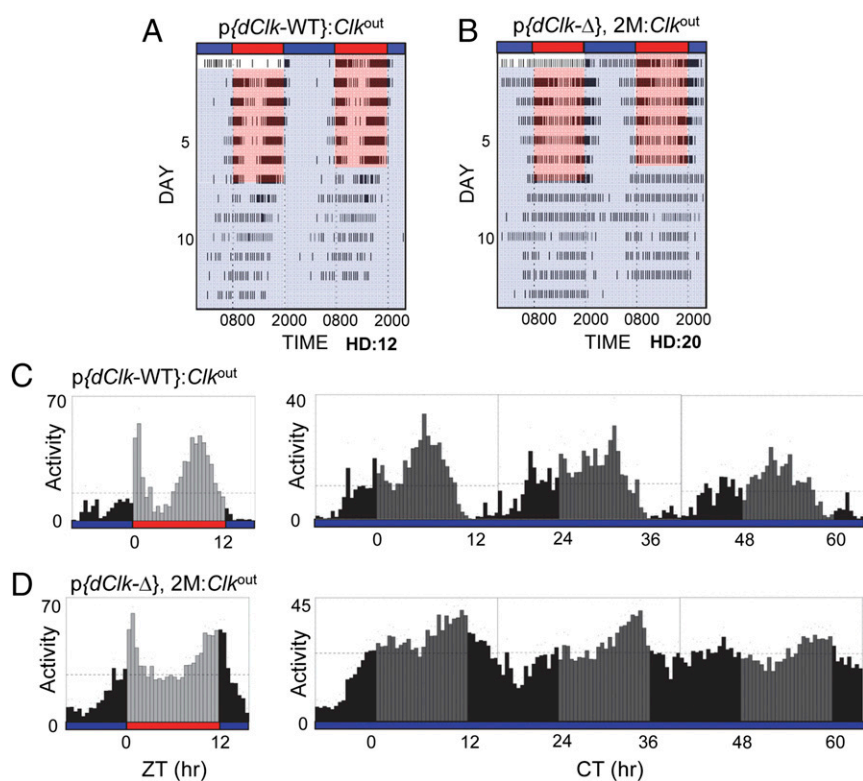
Fig. 9. p{*dClk-Δ*};*Clk*^out flies show anticipatory behavior and free-running rhythms in temperature cycle entrainment. Adult p{*dClk*-WT};*Clk*^out and p{*dClk-Δ*},2M;*Clk*^out flies were first exposed to continuous light for 2 d and entrained to a 12-h/12-h temperature cycle of 29 °C/24 °C in the dark for 6 d, followed by exposure to a constant temperature of 24 °C for 6 d. (*A* and *B*) Double-plotted actograms exhibit locomotor activity during the temperature cycle and at a constant temperature. The vertical black bars in each row represent fly activity. The red and blue horizontal bars indicate the thermo-phase and cryo-phase, respectively. (*C* and *D*) Daily activity profiles of each fly genotype. The gray vertical bars represent locomotor activity during the thermo-phase, and the black vertical bars represent locomotor activity during the cryo-phase of the temperature cycle. The dark gray vertical bars represent locomotor activity during the subjective thermo-phase.

domain within dCLK AA380–528. Thus, future studies will be required to delineate the direct PER binding domain on dCLK.

This study further reveals that the exon 19-encoded region of mCLK is essential for association with mPERs in mammalian cells (Fig. 1*F*). Previous studies have identified this region as the binding site of CLOCK-interacting protein, circadian (CIPC), a vertebrate-specific inhibitor of mCLK/BMAL1 (51, 52). CIPC also promotes the phosphorylation and subsequent destabilization of mCLK (51). In *Drosophila*, the association of PER via its CBD is required for the hyperphosphorylation and subsequent destabilization of dCLK (28, 36). Thus, CIPC and PER, although not homologous in sequence, share many similarities not only in their functions as repressors of circadian transcription but also in their posttranslational regulation of CLK proteins. Thus, it is plausible that PER or CIPC surfaces responsible for dCLK or mCLK interaction, respectively, are homologous. Also, based on the results of our in vitro binding assays performed with dCLK fragments, it will be interesting to explore whether the region of mCLK homologous to dCLK AA380–528 might function similarly as the direct binding domain for mPERs.

Similar to mCLKΔ19, dCLK-Δ showed compromised transcriptional activity in an E-box–dependent luciferase reporter assay in S2 cells, suggesting a role of AA657–707 in dCLK/CYC-dependent transcriptional activation (22, 32, 53) (Fig. 4 and Fig. S1). Indeed, in p{*dClk-Δ*};*Clk*^out flies, *tim*, *per*, and *vri* mRNA levels measured from whole heads were ~40% of the mRNA levels of control p{*dClk*-WT};*Clk*^out flies at the peak time point, suggesting that the transcriptional activity of the dCLK-Δ/CYC complex is compromised (Fig. 4 *A–C* and Fig. S3 *A* and *B*). Interestingly, despite the low levels of dCLK target mRNAs, including *tim*, *per*, and *vri*, in p{*dClk-Δ*};*Clk*^out flies compared with p{*dClk*-WT};*Clk*^out flies, TIM and PER protein levels measured from whole heads were comparable in the two groups of transgenic flies. However, TIM levels were maintained at peak level during the entire dark phase, indicating that TIM degradation was attenuated in p{*dClk-Δ*};*Clk*^out flies, which may also have stabilized PER against degradation (40–43). Inefficient TIM degradation during the dark phase might also have rendered TIM protein still detectable at

4 h after lights-on (Fig. 4*D*). Given that TIM and dCLK-Δ binding was also reduced in p{*dClk-Δ*};*Clk*^out flies (Fig. 5), we propose that robust light-independent TIM degradation might occur when TIM is in the PER/TIM/dCLK/CYC tetramer complex. It is possible that in p{*dClk-Δ*};*Clk*^out flies, newly translated PER/TIM accumulates without the degradation normally seen in p{*dClk*-WT};*Clk*^out flies to maintain steady-state levels of PER/TIM during the dark period. The attenuated degradation of PER/TIM likely explains the minor differences in protein levels despite pronounced differences in mRNA levels between p{*dClk*-WT};*Clk*^out and p{*dClk-Δ*};*Clk*^out flies. Nonetheless, light-dependent degradation of TIM seems to be intact in p{*dClk-Δ*};*Clk*^out flies, driving normal cycles in the abundance of TIM and PER during the photic cycle (Fig. 4). In the constant dark condition, however, TIM and PER accumulate more during the subjective day, leading to much dampened amplitudes of *tim* and *per* mRNA cycling, which ultimately result in behavioral arrhythmicity (Fig. S3). Together with the result that no rhythmic locomotor behaviors are observed in the LD cycle in p{*dClk-Δ*};*Clk*^out flies (Fig. 2), these results support the notion that the molecular oscillation of core clock proteins is necessary but not sufficient for behavioral rhythmicity. Given that dCLK/CYC activates not only the expression of core clock genes but also the expression of clock-controlled genes, it is possible that clock-controlled output genes are down-regulated, leading to behavioral arrhythmicity in p{*dClk-Δ*};*Clk*^out flies.

An unanticipated aspect of our research is that dCLK-Δ would differentially perturb the molecular clockwork in pacemaker-neuron subpopulations (Figs. 6 and 7). In p{*dClk-Δ*};*Clk*^out flies, dCLK target clock proteins, such as PER, TIM, and VRI, displayed pacemaker-neuron–dependent alterations (i.e., expression was reduced in LN_vs but not significantly in LN_ds and DNs in both photic and temperature cycles) (Figs. 6–8 and Figs. S4–S7). At the behavioral level, the p{*dClk-Δ*};*Clk*^out flies exhibited no morning and evening anticipation and arrhythmic free-running activity in the photic entrainment condition; however, they showed anticipatory behavior and improved free-running rhythms in the temperature entrainment condition (Figs. 2 and 9). Thus, the robust molecular oscillations in LN_ds and DNs of p{*dClk-Δ*};*Clk*^out flies can generate

behavioral rhythmicity in temperature entrainment conditions, but not in photic entrainment conditions. Importantly, previous reports demonstrate that DN_1-generated evening activity is suppressed by high-intensity light (20, 54) and enhanced by warm temperature (20). Therefore, it might be that DN-generated rhythmic outputs are suppressed in p{dClk-Δ};Clk[out] flies, resulting in arrhythmic behaviors under the standard (high-intensity light) photic entrainment condition used in this study. It is also important to note that several lines of evidence support the idea that DNs play important roles to control circadian behaviors in temperature entrainment conditions (18–21). Consistently, in p{dClk-Δ};Clk[out] flies, relatively intact molecular clockwork in DNs deduced from strong expression of dCLK target genes entrains to the temperature cycle, but with phase delay, and generates the delayed anticipatory behavior of temperature transition, ultimately contributing to improved free-running rhythms compared with the rhythms under photic cycle entrainment conditions.

Given that dCLK-Δ showed reduced transactivation of dCLK target genes, we investigated whether reduction in transcriptional activity such as seen in p{dClk-Δ};Clk[out] flies might have lesser effects on locomotor behavior in temperature cycles than in photic cycles. Flies harboring Clk[ar], a hypomorphic allele of dClk, show compromised dCLK activity and levels leading to behavioral arrhythmicity under photic conditions, albeit with persistent but reduced amplitudes in PER and TIM molecular rhythms (55). Thus, we compared circadian locomotor behaviors of Clk[ar] in the photic and temperature entrainment conditions. Unlike p{dClk-Δ};Clk[out] flies, Clk[ar] flies displayed no anticipatory activity of temperature transition and showed arrhythmicity under both entrainment conditions (Fig. S8). This observation suggests that the reduction in transcriptional activity of dCLK itself does not necessarily impose less of an effect on behavioral rhythms in temperature cycles than in photic cycles. Nonetheless, the possibility remains that the extent of the reduction in transcriptional activity of Clk[ar] is greater than the extent of the reduction in transcriptional activity of dCLK-Δ, leading to arrhythmic behavior under photic and temperature cycle conditions.

In p{dClk-Δ};Clk[out] flies, the LN_v-specific reduction in dCLK target protein expression likely resulted from compromised transcription, because all of the evaluated dCLK target proteins in separate loops of the TTFL (e.g., TIM, PER, VRI) displayed reduced expression in LN_vs. What would lead to these pacemaker-neuron–dependent alterations in clock protein abundances in p{dClk-Δ};Clk[out] flies? Given that the AA657–707 region of dCLK may play roles in interactions with multiple factors, it is tempting to speculate that cell type-specific circadian transcriptional activation occurs via the engagement of cell type-specific transcriptional coactivators and/or other transcription factors through this domain. Interestingly, in tissue-specific circadian transcription programs, context-dependent transcription factors recruit the dCLK/CYC complexes to actively transcribed genes by binding to target enhancer elements (56). Our results further suggest that although dCLK/CYC plays a central role in circadian transcription, the exact functional architecture of dCLK/CYC-containing transcriptional complexes is cell type-specific. Our current hypothesis is that LN_v-specific coactivators and/or transcription factors are required for dCLK/CYC-dependent transcriptional activation in LN_vs and that these associations are mediated through the AA657–707 domain of dCLK. In contrast, factors associated via dCLK AA657–707 might not be required for circadian transcription in LN_ds and DNs, or the association between factors and dCLK might involve other regions of dCLK in those neurons. Future studies will be required to address the mechanisms underlying cell-specific circadian transcription.

Animals exhibit direct light-induced responses called masking. In positive masking, dim light increases activity, and in negative masking, bright light suppresses activity (46, 47). Our results showed that p{dClk-Δ};Clk[out] flies exhibited reduced responses to both masking effects, because the lights-on/off transition-induced startle response was very weak (or absent), and the suppression of activity induced by constant light exposure was insignificant (Figs. 2 and 8). The role of dCLK in light-mediated responses has been reported previously (35, 55, 57, 58). Given that dCLK-Δ exhibited robust defect in LN_vs in our study, intact dCLK in light-sensitive LN_vs might be more relevant for masking responses. Interestingly, Clk/Clk mice show reduced masking in responses to light (59–61). Taken together, these data suggest that light-induced direct behavioral responses in Drosophila and mice might use a similar underlying mechanism.

In summary, our results demonstrate that the AA657–707 region of dCLK and the region encoded by exon 19 of mCLK are essential for PER interaction and circadian transactivation. The p{dClk-Δ};Clk[out] flies manifested more pronounced defects in standard photic cycle-induced circadian behavior, which was accompanied by more severe perturbations in molecular clockwork in LN_vs than in DNs. Based on these intriguing observations, we propose that the dCLK/CYC-controlled TTFL operates differently depending on the cellular context, which likely endows pacemaker neurons with distinct circadian attributes, such as varying sensitivity to light- and temperature-entraining cues.

Materials and Methods

All materials and methods used in this study are detailed in *SI Materials and Methods*. Materials include plasmids, fly strains, and antibodies. Methods include generation of *dClkΔ657–707*-expressing transgenic flies, behavioral analyses, quantitative real-time PCR, immunoblotting, immunofluorescence analysis, and in vitro binding assays.

1. Hardin PE (2011) Molecular genetic analysis of circadian timekeeping in Drosophila. *Adv Genet* 74:141–173.
2. Mohawk JA, Green CB, Takahashi JS (2012) Central and peripheral circadian clocks in mammals. *Annu Rev Neurosci* 35:445–462.
3. Cyran SA, et al. (2003) vrille, Pdp1, and dClock form a second feedback loop in the Drosophila circadian clock. *Cell* 112(3):329–341.
4. Glossop NR, et al. (2003) VRILLE feeds back to control circadian transcription of Clock in the Drosophila circadian oscillator. *Neuron* 37(2):249–261.
5. Partch CL, Green CB, Takahashi JS (2014) Molecular architecture of the mammalian circadian clock. *Trends Cell Biol* 24(2):90–99.
6. Grima B, Chélot E, Xia R, Rouyer F (2004) Morning and evening peaks of activity rely on different clock neurons of the Drosophila brain. *Nature* 431(7010):869–873.
7. Ripperger JA, Schibler U (2006) Rhythmic CLOCK-BMAL1 binding to multiple E-box motifs drives circadian Dbp transcription and chromatin transitions. *Nat Genet* 38(3):369–374.
8. Stoleru D, Peng Y, Agosto J, Rosbash M (2004) Coupled oscillators control morning and evening locomotor behaviour of Drosophila. *Nature* 431(7010):862–868.
9. Chung BY, Kilman VL, Keath JR, Pitman JL, Allada R (2009) The GABA(A) receptor RDL acts in peptidergic PDF neurons to promote sleep in Drosophila. *Curr Biol* 19(5):386–390.
10. Shang Y, Griffith LC, Rosbash M (2008) Light-arousal and circadian photoreception circuits intersect at the large PDF cells of the Drosophila brain. *Proc Natl Acad Sci USA* 105(50):19587–19594.
11. Sheeba V, et al. (2008) Large ventral lateral neurons modulate arousal and sleep in Drosophila. *Curr Biol* 18(20):1537–1545.
12. Sheeba V, Fogle KJ, Holmes TC (2010) Persistence of morning anticipation behavior and high amplitude morning startle response following functional loss of small ventral lateral neurons in Drosophila. *PLoS One* 5(7):e11628.
13. Rieger D, Shafer OT, Tomioka K, Helfrich-Förster C (2006) Functional analysis of circadian pacemaker neurons in Drosophila melanogaster. *J Neurosci* 26(9):2531–2543.
14. Yoshii T, Rieger D, Helfrich-Förster C (2012) Two clocks in the brain: An update of the morning and evening oscillator model in Drosophila. *Prog Brain Res* 199:59–82.
15. Glaser FT, Stanewsky R (2005) Temperature synchronization of the Drosophila circadian clock. *Curr Biol* 15(15):1352–1363.
16. Pittendrigh CS (1954) On temperature independence in the CLOCK system controlling emergence time in Drosophila. *Proc Natl Acad Sci USA* 40(10):1018–1029.
17. Yoshii T, Sakamoto M, Tomioka K (2002) A temperature-dependent timing mechanism is involved in the circadian system that drives locomotor rhythms in the fruit fly Drosophila melanogaster. *Zoolog Sci* 19(8):841–850.

18. Miyasako Y, Umezaki Y, Tomioka K (2007) Separate sets of cerebral clock neurons are responsible for light and temperature entrainment of Drosophila circadian locomotor rhythms. *J Biol Rhythms* 22(2):115–126.

19. Busza A, Murad A, Emery P (2007) Interactions between circadian neurons control temperature synchronization of Drosophila behavior. *J Neurosci* 27(40):10722–10733.

20. Zhang Y, Liu Y, Bilodeau-Wentworth D, Hardin PE, Emery P (2010) Light and temperature control the contribution of specific DN1 neurons to Drosophila circadian behavior. *Curr Biol* 20(7):600–605.

21. Picot M, Klarsfeld A, Chélot E, Malpel S, Rouyer F (2009) A role for blind DN2 clock neurons in temperature entrainment of the Drosophila larval brain. *J Neurosci* 29(26): 8312–8320.

22. Darlington TK, et al. (1998) Closing the circadian loop: CLOCK-induced transcription of its own inhibitors per and tim. *Science* 280(5369):1599–1603.

23. Lee C, Bae K, Edery I (1998) The Drosophila CLOCK protein undergoes daily rhythms in abundance, phosphorylation, and interactions with the PER-TIM complex. *Neuron* 21(4):857–867.

24. Chen R, et al. (2009) Rhythmic PER abundance defines a critical nodal point for negative feedback within the circadian clock mechanism. *Mol Cell* 36(3):417–430.

25. Kiyohara YB, et al. (2006) The BMAL1 C terminus regulates the circadian transcription feedback loop. *Proc Natl Acad Sci USA* 103(26):10074–10079.

26. Menet JS, Abruzzi KC, Desrochers J, Rodriguez J, Rosbash M (2010) Dynamic PER repression mechanisms in the Drosophila circadian clock: From on-DNA to off-DNA. *Genes Dev* 24(3):358–367.

27. Sato TK, et al. (2006) Feedback repression is required for mammalian circadian clock function. *Nat Genet* 38(3):312–319.

28. Sun WC, et al. (2010) Two distinct modes of PERIOD recruitment onto dCLOCK reveal a novel role for TIMELESS in circadian transcription. *J Neurosci* 30(43):14458–14469.

29. Chang DC, Reppert SM (2003) A novel C-terminal domain of drosophila PERIOD inhibits dCLOCK:CYCLE-mediated transcription. *Curr Biol* 13(9):758–762.

30. King DP, et al. (1997) The mouse Clock mutation behaves as an antimorph and maps within the W19H deletion, distal of Kit. *Genetics* 146(3):1049–1060.

31. Chang DC, et al. (2003) Constructing a feedback loop with circadian clock molecules from the silkmoth, Antheraea pernyi. *J Biol Chem* 278(40):38149–38158.

32. Shimomura K, et al. (2013) Usf1, a suppressor of the circadian Clock mutant, reveals the nature of the DNA-binding of the CLOCK:BMAL1 complex in mice. *eLife* 2:e00426.

33. Lee E, et al. (2014) Phosphorylation of a central clock transcription factor is required for thermal but not photic entrainment. *PLoS Genet* 10(8):e1004545.

34. Mahesh G, et al. (2014) Phosphorylation of the transcription activator CLOCK regulates progression through a ∼ 24-h feedback loop to influence the circadian period in Drosophila. *J Biol Chem* 289(28):19681–19693.

35. Allada R, White NE, So WV, Hall JC, Rosbash M (1998) A mutant Drosophila homolog of mammalian Clock disrupts circadian rhythms and transcription of period and timeless. *Cell* 93(5):791–804.

36. Kim EY, Edery I (2006) Balance between DBT/CKIepsilon kinase and protein phosphatase activities regulate phosphorylation and stability of Drosophila CLOCK protein. *Proc Natl Acad Sci USA* 103(16):6178–6183.

37. Yu W, Zheng H, Houl JH, Dauwalder B, Hardin PE (2006) PER-dependent rhythms in CLK phosphorylation and E-box binding regulate circadian transcription. *Genes Dev* 20(6):723–733.

38. Kim EY, Ko HW, Yu W, Hardin PE, Edery I (2007) A DOUBLETIME kinase binding domain on the Drosophila PERIOD protein is essential for its hyperphosphorylation, transcriptional repression, and circadian clock function. *Mol Cell Biol* 27(13):5014–5028.

39. Yu W, Zheng H, Price JL, Hardin PE (2009) DOUBLETIME plays a noncatalytic role to mediate CLOCK phosphorylation and repress CLOCK-dependent transcription within the Drosophila circadian clock. *Mol Cell Biol* 29(6):1452–1458.

40. Ko HW, Jiang J, Edery I (2002) Role for Slimb in the degradation of Drosophila Period protein phosphorylated by Doubletime. *Nature* 420(6916):673–678.

41. Price JL, et al. (1998) Double-time is a novel Drosophila clock gene that regulates PERIOD protein accumulation. *Cell* 94(1):83–95.

42. Price JL, Dembinska ME, Young MW, Rosbash M (1995) Suppression of PERIOD protein abundance and circadian cycling by the Drosophila clock mutation timeless. *EMBO J* 14(16):4044–4049.

43. Suri V, Lanjuin A, Rosbash M (1999) TIMELESS-dependent positive and negative autoregulation in the Drosophila circadian clock. *EMBO J* 18(3):675–686.

44. Myers MP, Wager-Smith K, Rothenfluh-Hilfiker A, Young MW (1996) Light-induced degradation of TIMELESS and entrainment of the Drosophila circadian clock. *Science* 271(5256):1736–1740.

45. Zeng H, Qian Z, Myers MP, Rosbash M (1996) A light-entrainment mechanism for the Drosophila circadian clock. *Nature* 380(6570):129–135.

46. Golombek DA, Rosenstein RE (2010) Physiology of circadian entrainment. *Physiol Rev* 90(3):1063–1102.

47. Mrosovsky N (1999) Masking: History, definitions, and measurement. *Chronobiol Int* 16(4):415–429.

48. Boothroyd CE, Wijnen H, Naef F, Saez L, Young MW (2007) Integration of light and temperature in the regulation of circadian gene expression in Drosophila. *PLoS Genet* 3(4):e54.

49. Saunders DS (2002) *Insect Clocks* (Elsevier, Amsterdam), 3rd Ed.

50. Huang N, et al. (2012) Crystal structure of the heterodimeric CLOCK:BMAL1 transcriptional activator complex. *Science* 337(6091):189–194.

51. Yoshitane H, et al. (2009) Roles of CLOCK phosphorylation in suppression of E-box-dependent transcription. *Mol Cell Biol* 29(13):3675–3686.

52. Zhao WN, et al. (2007) CIPC is a mammalian circadian clock protein without invertebrate homologues. *Nat Cell Biol* 9(3):268–275.

53. Lowrey PL, Takahashi JS (2011) Genetics of circadian rhythms in mammalian model organisms. *Adv Genet* 74:175–230.

54. Zhang L, et al. (2010) DN1(p) circadian neurons coordinate acute light and PDF inputs to produce robust daily behavior in Drosophila. *Curr Biol* 20(7):591–599.

55. Allada R, Kadener S, Nandakumar N, Rosbash M (2003) A recessive mutant of Drosophila Clock reveals a role in circadian rhythm amplitude. *EMBO J* 22(13):3367–3375.

56. Meireles-Filho AC, Bardet AF, Yáñez-Cuna JO, Stampfel G, Stark A (2014) cis-regulatory requirements for tissue-specific programs of the circadian clock. *Curr Biol* 24(1):1–10.

57. Lu B, Liu W, Guo F, Guo A (2008) Circadian modulation of light-induced locomotion responses in Drosophila melanogaster. *Genes Brain Behav* 7(7):730–739.

58. Kim EY, et al. (2002) Drosophila CLOCK protein is under posttranscriptional control and influences light-induced activity. *Neuron* 34(1):69–81.

59. Redlin U, Hattar S, Mrosovsky N (2005) The circadian Clock mutant mouse: Impaired masking response to light. *J Comp Physiol A Neuroethol Sens Neural Behav Physiol* 191(1):51–59.

60. Spoelstra K, Oklejewicz M, Daan S (2002) Restoration of self-sustained circadian rhythmicity by the mutant clock allele in mice in constant illumination. *J Biol Rhythms* 17(6):520–525.

61. Vitaterna MH, et al. (2006) The mouse Clock mutation reduces circadian pacemaker amplitude and enhances efficacy of resetting stimuli and phase-response curve amplitude. *Proc Natl Acad Sci USA* 103(24):9327–9332.

62. Kume K, et al. (1999) mCRY1 and mCRY2 are essential components of the negative limb of the circadian clock feedback loop. *Cell* 98(2):193–205.

63. Jeong K, et al. (2015) Dual attenuation of proteasomal and autophagic BMAL1 degradation in Clock Δ19/+ mice contributes to improved glucose homeostasis. *Sci Rep* 5:12801.

64. Groth AC, Fish M, Nusse R, Calos MP (2004) Construction of transgenic Drosophila by using the site-specific integrase from phage phiC31. *Genetics* 166(4):1775–1782.

65. Venken KJ, He Y, Hoskins RA, Bellen HJ (2006) P[acman]: A BAC transgenic platform for targeted insertion of large DNA fragments in D. melanogaster. *Science* 314(5806): 1747–1751.

66. Sidote D, Majercak J, Parikh V, Edery I (1998) Differential effects of light and heat on the Drosophila circadian clock proteins PER and TIM. *Mol Cell Biol* 18(4):2004–2013.